PHYSICAL REVIEW B

SOLID STATE

THIRD SERIES, VOL. 3, NO. 9 1 MAY 1971

Mössbauer Spectroscopy with ^{61}Ni in Nickel–Transition-Metal Alloys and Nickel Compounds*

John C. Love,† Felix E. Obenshain, and Gordon Czjzek‡
Oak Ridge National Laboratory, Oak Ridge, Tennessee 37830
(Received 13 November 1970)

Nuclear γ resonance spectra have been observed with 67.4-keV γ rays of ^{61}Ni in Cu-Ni, Co-Ni, and Fe-Ni alloy absorbers and in some nickel-compound absorbers. The source contained the parent isotope ^{61}Co, produced by the reaction ^{64}Ni$(p, \alpha)^{61}$Co, in a nonmagnetic $^{64}Ni_{0.86}V_{0.14}$ alloy. Source and absorber were held at 4.2 °K. The magnetic moment of the 67.4-keV state of ^{61}Ni, $\mu(67.4) = (+0.481 \pm 0.006)\mu_N$ was determined to a better precision than by earlier measurements. Limits were placed on the value of the fractional change in charge radius $(\Delta R/R)_N$ of the 67.4-keV state compared to the ground-state radius, $-1.8\times10^{-4} \leq (\Delta R/R)_N \leq -0.7\times10^{-4}$. The concentration dependence of the average magnetic hyperfine field at ^{61}Ni nuclei in Ni-Fe, Ni-Co, and in Ni-Cu alloys is very nearly proportional to that of the bulk alloy magnetization. Absolute values of the hyperfine field in antiferromagnetic Ni^{2+} compounds agree wtih the results of unrestricted Hartree-Fock calculations. We have deduced isomer shifts from the measured energy shifts after subtracting second-order Doppler-shift contributions. The results are compared with values of electron densities at ^{61}Ni nuclei obtained from relativistic Hartree-Slater-Latter calculations.

I. INTRODUCTION

We have employed nuclear γ resonance (NGR) spectroscopy with γ rays of energy $E_\gamma = 67.4$ keV, emitted by ^{61}Ni in the transition from the first excited state to the ground state, in an investigation of hyperfine interactions at ^{61}Ni nuclei in 3*d* transition-metal alloys and in several ionic compounds. Difficulties associated with source production (short half-life for parent isotopes), high γ-ray energy, lifetime of the excited state [$\tau = (7.3 \pm 0.3)\times10^{-9}$ sec], and the spin sequence ($I_e = \frac{5}{2}$; $I_g = \frac{3}{2}$) have delayed the exploitation of the potential of ^{61}Ni NGR spectroscopy after the first observation of the Mössbauer effect with this nucleus.[1] Among the 3*d* transition elements, ^{61}Ni is the only nucleus besides ^{57}Fe suitable for NGR spectroscopy. Observation of hyperfine interactions at ^{57}Fe nuclei by NGR has contributed to the understanding of properties such as electronic and magnetic configuration of iron ions in compounds,[2,3] the formation of local moments at iron atoms in alloys,[3,4] and others. Since many properties associated with nickel in alloys and compounds differ significantly from those of iron in analogous materials, the observation of hyperfine interactions at ^{61}Ni is an important complement to the work with ^{57}Fe in the development of the physics and chemistry of transition elements.

The principal objective of the present experiments was the measurement of magnetic hyperfine fields and electronic charge densities at ^{61}Ni nuclei in 3*d* transition-metal alloys (Fe-Ni, Co-Ni, and Cu-Ni). The determination of the excited-state charge radius, which is needed to deduce electronic charge densities from isomer shifts, required further measurements in ionic nickel compounds.

In contrast to most other methods which measure quantities related to the electronic structure of alloys, measurements of hyperfine interactions at nuclear probes [NGR, NMR, perturbed angular correlation (PAC)] provide specific information about electronic parameters associated with individual alloy components as they are influenced by alloy composition. Thus, the information content of results obtained by nuclear methods is in this respect more selective than that of other experimental data. However, one has to be cautious when interpreting results obtained with nuclear species doped into an alloy in terms of bulk alloy properties. For example, NGR data have been obtained with several probe nuclei (^{57}Fe,[5] ^{197}Au,[6] and ^{119}Sn[7]) in Cu-Ni alloys, but from these results it is diffi-

cult to draw direct conclusions regarding changes in the population of Ni $3d$ and $4s$ states which would be of interest for comparison with theoretical models of the electronic structure of this alloy system.[8]

We discuss in Sec. II the dominant contributions to hyperfine interactions in the materials that we have studied, the approach that we have used in deducing quantities relating to electronic structure, and the nuclear parameters of ^{61}Ni of importance for the analysis. In Sec. III experimental details are described, in Sec. IV we present the results of ^{61}Ni NGR obtained in $3d$ transition-metal alloys, and in Sec. V those obtained with ionic compounds. Preliminary reports[9] of parts of this work have been given.

II. HYPERFINE INTERACTIONS AND NUCLEAR PROPERTIES OF ^{61}Ni

The Hamiltonian of a solid contains terms due to the electromagnetic interaction between nuclei and electrons. The effect on nuclear energy levels which are observed in NGR spectra can be described in first order by the multipole expansion.[10] We consider only the leading terms of this expansion, the monopole interaction between nuclear and electronic charges, and the magnetic dipole interaction. The electric quadrupole interaction must, in general, be included, but in our present investigations we found a weak indication of its occurrence only in one compound (NiF_2) which gave at best a qualitative estimate of the interaction strength.

The electric monopole interaction leads to a shift δ_{IS} of the emitted or absorbed γ-ray energy (isomer shift) which is given approximately by[11]

$$\delta_{IS} = K(\Delta R/R)_N \rho_{el}(0), \tag{1}$$

where

$$K = (4\pi c Z e^2/5E_\gamma)\, R_N^2 = 1.12\times10^{-24}\ \text{cm}^4/\text{sec} \quad \text{for } ^{61}\text{Ni}.$$

$(\Delta R/R)_N = (R_N^{Ex\,S} - R_N^{GS})/R_N^{GS}$ is the relative difference of the rms nuclear charge radii, and $e\rho_{el}(0)$ is the electronic charge density at the nuclei. This equation involves the approximation of a spherical uniformly charged nucleus. If electronic charge densities are derived from nonrelativistic wave functions, a correction factor $S'(Z)$ must be applied.[12]

The contribution of the magnetic dipole interaction to the Hamiltonian can be written in the form

$$H_{M1} = -\vec{\mu}\cdot\vec{H}_{hf}, \tag{2}$$

where $\vec{\mu}$ is the nuclear magnetic moment, and $\vec{H}_{hf}$ is the effective magnetic field at the nucleus generated by electron currents and spins. This interaction lifts the $(2j+1)$-fold degeneracy of a nuclear energy level of spin j and results in a splitting of the NGR spectrum.

A. Electronic Charge Densities and Magnetic Hyperfine Fields

The isomer shift δ_{IS} as given in Eq. (1) is proportional to the product of two unknown parameters $(\Delta R/R)_N$ and $\rho_{el}(0)$. The present status of nuclear theory does not permit a reliable estimate of $(\Delta R/R)_N$. This quantity can be determined experimentally by isomer-shift measurements (electronic or μ mesic[13]) if the charge density $e\rho_{el}(0)$ or $e\rho_\mu(0)$ is known. Measurements of μ-mesic isomer shifts for ^{61}Ni have not been reported, and we base our estimate of $(\Delta R/R)_N$ on NGR data of electronic shifts.

Values of electronic charge densities have been calculated by several authors[14–18] whose approaches differ in degree of sophistication in the various problem areas of such calculations (treatment of exchange and correlations, relativistic vs nonrelativistic calculation, etc.). Electronic wave functions from which $\rho_{el}(0)$ can be extracted have been published almost exclusively for free atoms or ions. NGR isomer shifts are measured with nuclei in solids, and the use of free-ion wave functions in the analysis of these data introduces some uncertainty.

In our analysis we use charge-density values computed with a series of programs (RELWAV)[17] which calculate relativistic electronic wave functions in the Hartree-Slater-Latter approximation, in one version for free ions, in another version with Wigner-Seitz boundary conditions which are at least one step toward a realistic calculation of wave functions in solids. The total electronic densities at ^{61}Ni nuclei computed for several values of the Wigner-Seitz radius r_{WS} and with free-ion boundary conditions are listed in Table I. We compare in Sec. V A our experimental isomer-shift data with the density values obtained with $r_{WS} = 1.404\times10^{-8}$ cm, the value appropriate for metallic nickel. A graphical representation of calculated electron densities and a comparison with experimental isomer shifts is given in the form of a Panek-Perlow plot[16] in Fig. 5.

In the case of metallic nickel the Wigner-Seitz boundary condition is a good approximation for wave functions of the core electrons and for conduction electrons (derived from $3d$ and $4s$ atomic states) with wave vector $\vec{k} = 0$. For the ionic compounds the Wigner-Seitz approximation is expected to give only approximate values. The molecular-orbital Hartree-Fock calculations of the electronic structure of atomic clusters [for example, the work of Ellis, Freeman, and Ros[19] on $(NiF_6)^{4-}$ with parameters corresponding to $KNiF_3$] could be applied to an analysis of measurements in these compounds, but no parameters relevant to hyperfine interactions at nickel have been reported.

In solid-state theory, calculations are in general done in a nonrelativistic approximation. As pointed out earlier, relativistic effects on the electron wave function at the nucleus can be accounted for by introducing the factor $S'(Z)$ which has the value 1.34

TABLE I. Relativistic electron densities at ^{61}Ni nuclei, $\rho_{el}(0)$ in units 10^{26} cm^{-3}, calculated with WS boundary conditions (columns 2–7, r_{WS} is the WS radius in units 10^{-8} cm), and for free ions (column 8).

Configuration \ r_{WS}	0.529	1.058	1.404	1.587	2.117	10.583	Free ions
$3d^6 4s^0$	1326.6427	1330.4836	1330.2733	1330.2363	1330.2220	1330.2219	1330.2507
$4s^1$	1344.5295	1332.1426	1331.1473	1331.0516	1331.2612	1331.4080	1331.3023
$4s^2$	•••	1333.7381	1331.8778	1331.6744	1331.9578	1332.3035	1332.1706
$3d^7 4s^0$	1326.2544	1330.1965	1329.9518	1329.8862	1329.8455	1329.8436	1329.8914
$4s^1$	1344.2403	1331.8760	1330.7626	1330.5816	1330.6062	1330.8137	1330.7162
$4s^2$	1362.3764	1333.4912	1331.4475	1331.1200	1331.0653	1331.4848	1331.3598
$3d^8 4s^0$	1325.9221	1330.0057	1329.7628	1329.6823	1329.6019	1329.5813	1329.6346
$4s^1$	1344.9689	1331.6851	1330.5222	1330.2853	1330.1210	1330.3286	1330.2390
$4s^2$	1362.1719	1333.3164	1331.1758	1330.7751	1330.4375	1330.7789	1330.6631
$3d^9 4s^0$	1325.5884	1329.8633	1329.6837	1329.5868	1329.4692	1329.4406	1329.4797
$4s^1$	1343.7124	1331.5498	1330.3888	1330.1296	1329.8496	1329.9547	1329.8768
$4s^2$	•••	•••	1331.0145	•••	•••	•••	•••
$3d^{10} 4s^0$	•••	1329.7635	1329.6581	1329.5690	1329.4456	1329.3892	1329.4169
$4s^1$	1343.4675	1331.4548	1330.3230	1330.0622	1329.7329	•••	•••
$4s^2$	•••	•••	1330.9218	•••	•••	•••	•••

for nickel.[12] As an illustration of the relative importance of relativistic and boundary condition effects, we compare in Table II the electron density $\rho_{el}(0)$ of one $4s$ electron in nickel atoms with configurations $3d^8 4s^2$ and $3d^9 4s^1$ (a) computed from the wave functions of Herman and Skillman[15] multiplied by $S'(28) = 1.34$, (b) computed with RELWAV and free-atom boundary conditions, and (c) computed with RELWAV and $r_{WS} = 1.404 \times 10^{-8}$ cm.

As discussed extensively in the literature[20,21] there are three sources of magnetic hyperfine fields: (i) the contact field which is proportional to the unpaired spin density at the nucleus, (ii) the orbital field caused by electrons in states of nonzero angular momentum, and (iii) the spin-dipole field which originates in the dipole-dipole interaction between nuclear and electronic spins and vanishes at sites of cubic symmetry. The contact term (i) is usually subdivided into contributions from core polarization and those from unpaired valence and conduction electrons. The core-polarization field for Ni^{2+} ions has been calculated by Watson and Freeman.[22]

TABLE II. Electron density of one $4s$ electron at ^{61}Ni nuclei in nickel atoms in units 10^{26} cm^{-3}, (a) from the wave functions of Herman and Skillman, multiplied by $S'(28) = 1.34$, (b) computed with RELWAV and free-atom boundary conditions, and (c) computed with RELWAV and $r_{WS} = 1.404 \times 10^{-8}$ cm.

Configuration	$3d^8 4s^2$	$3d^9 4s^1$
$\rho_{4s}^{(a)}(0)$	0.519	0.381
$\rho_{4s}^{(b)}(0)$	0.534	0.403
$\rho_{4s}^{(c)}(0)$	0.679	0.667

B. Nuclear Parameters of ^{61}Ni

NGR spectra are characterized by properties of the nuclear states involved in the γ-ray transition as well as by the environment of the probe nuclei, and information on nuclear parameters can be deduced from NGR spectra. Most of the relevant nuclear parameters of ^{61}Ni have been measured by other methods and are compiled by Muir *et al.*[23] When our experiments began, the value of the magnetic moment of the 67.4-keV state was known,[24] but with relatively large uncertainty. No measurements of $(\Delta R/R)_N$ and of the excited-state quadrupole moment had been reported.

The largest magnetic hyperfine field at ^{61}Ni, and hence the best resolution of NGR spectra found in this investigation, was obtained with dilute solutions of ^{61}Ni in Fe (Fig. 1). The magnetic moment of the 67.4-keV state $\mu(67.4) = (+0.481 \pm 0.006)\mu_N$ was deduced from a least-squares fit of the spectrum (see Sec. III C) in conjunction with the value $\mu_g = (-0.749 \pm 0.007)\mu_N$ for the ground-state moment.[25] This value of $\mu(67.4)$ agrees very well with that deduced from Mössbauer spectra in Ref. 24 and with that obtained by Erich,[26] but it is different from the preliminary results published by Love *et al.*[27]

A value of $(\Delta R/R)_N$ could not be extracted from a single Mössbauer spectrum, and we discuss the experimental data and the considerations employed in deriving an estimate of this parameter in Sec. V A. The result is that the value $(\Delta R/R)_N$ lies in the range $-1.8 \times 10^{-4} \leq (R/R)_N \leq -0.7 \times 10^{-4}$.

For the quadrupole moment of the excited state we can give only a preliminary estimate, $Q_e = (0.05 \pm 0.15) \times 10^{-24}$ cm^2, derived from a fit to the spectrum of a NiF_2 absorber (Sec. V B, Fig. 7) and the value $Q_g = (+0.162 \pm 0.015) \times 10^{-24}$ cm^2 for the

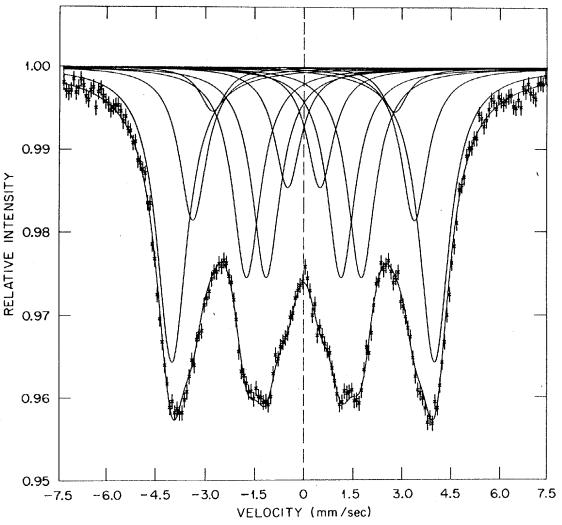

FIG. 1. Mössbauer spectrum obtained with the source ^{61}Co in a nonmagnetic $^{64}Ni_{0.86}V_{0.14}$ alloy, and a $Fe_{0.95}Ni_{0.05}$ absorber at 4.2 °K, fitted with the Mössbauer transmission integral.

ground-state quadrupole moment.[28]

Theoretical efforts to calculate values of the nuclear parameters discussed above have been successful in some cases. Thus, for example, the quasiparticle theory of Migdal[29] yields good values for magnetic moments, and calculations of $(\Delta R/R)_N$ in the framework of the pairing plus quadrupole model of Sorensen,[30] in general, agree with experimental values.

III. EXPERIMENTAL DETAILS

A. Materials

Several methods for populating the first excited state of the ^{61}Ni nucleus are possible. These methods may be grouped into three classes: (i) those which use ^{61}Co as the β^- decay precursor ($T_{1/2}$ = 99 min), (ii) those leading to ^{61}Cu which decays by electron capture and positron emission to ^{61}Ni ($T_{1/2}$ = 200 min), and (iii) Coulomb excitation and nuclear reactions which directly populate the first excited level of ^{61}Ni. For the present experiment we used a method of the first type, producing ^{61}Co by the reaction ^{64}Ni(p, α)^{61}Co with 22-MeV protons. Nonmagnetic sources were prepared in the form of an alloy of ^{64}Ni with 14-at.% vanadium. The powdered alloy was pressed into aluminum disks which served as target backings for the cyclotron irradiations. Since these powder targets showed effects of radiation damage (broadening of the NGR linewidth) after about 500 μA h of irradiation, we changed at a later stage of the experiments to 0.1-mm-thick $^{64}Ni_{0.86}V_{0.14}$ alloy foil targets which could withstand a proton beam current of 5–10 μA. The activated sources could be mounted in a Mössbauer spectrometer without further treatment.

The recoilless-emission spectrum of a $^{64}Ni_{0.86}V_{0.14}$ alloy source at 4.2 °K was determined from a series of Mössbauer spectra taken with nonmagnetic $Ni_{0.86}V_{0.14}$ absorbers which varied in thickness and ^{61}Ni enrichment. The recoilless fraction of the source was found to be $f_s = (16.2 \pm 0.3)\%$, the width of the emission line was $\Gamma_s = (0.42 \pm 0.03)$ mm/sec, which may be compared with $\Gamma_{nat} = (0.401 \pm 0.016)$ mm/sec derived from the electronically measured mean life of the 67.4-keV excited state.[31] The corresponding parameters of the absorbers were the same within experimental uncertainty.

Alloys of nickel with copper, iron, and cobalt, used as absorbers, were prepared by arc melting the appropriate mixtures of pure metal powder. Specimens with less than 50-at.% nickel were doped with ^{61}Ni. To ensure homogeneity, the alloy buttons were heat treated in vacuum or in an inert atmosphere. The buttons were then rolled to the desired absorber thickness of 0.25–0.50 mm. Chemical and electron microprobe analyses to test for composition and macroscopic homogeneity were obtained for all samples.

The compounds of Ni that were studied were either obtained from commerical suppliers or prepared in the laboratory. The purity and structure of the materials were examined by chemical and x-ray analyses. Absorbers were prepared by binding the powdered material in Epoxy. Because of the instability of $K_4Ni_2(CN)_6$ in air, it was prepared and sealed in a nylon cell under an atmosphere of He gas.

B. Mössbauer Spectrometer

The spectrometer was based on a design by Kankeleit.[32] The spectrum was stored in a multichannel analyzer (MCA) operated in the time mode in which the channels are opened and closed sequentially by pulses provided from an external pulse generator. The square wave, which originates from the most significant bit of the address register of the MCA, correlated precisely the motion of the transducer with time scan of the MCA. The velocity of the transducer was determined by a triangular wave derived from the bistable square wave. A diagram of the electronic circuit is presented in Fig. 2. The entire velocity range is scanned twice during each period of the wave, and the data for motion towards the absorber and motion away from the absorber are stored consecutively in the two halves of the MCA.

The linearity of the velocity–channel-number conversion depends on (i) the linearity of the reference triangle, (ii) the degree to which the transducer armature can be forced to follow the reference signal, and (iii) the linearity of the velocity

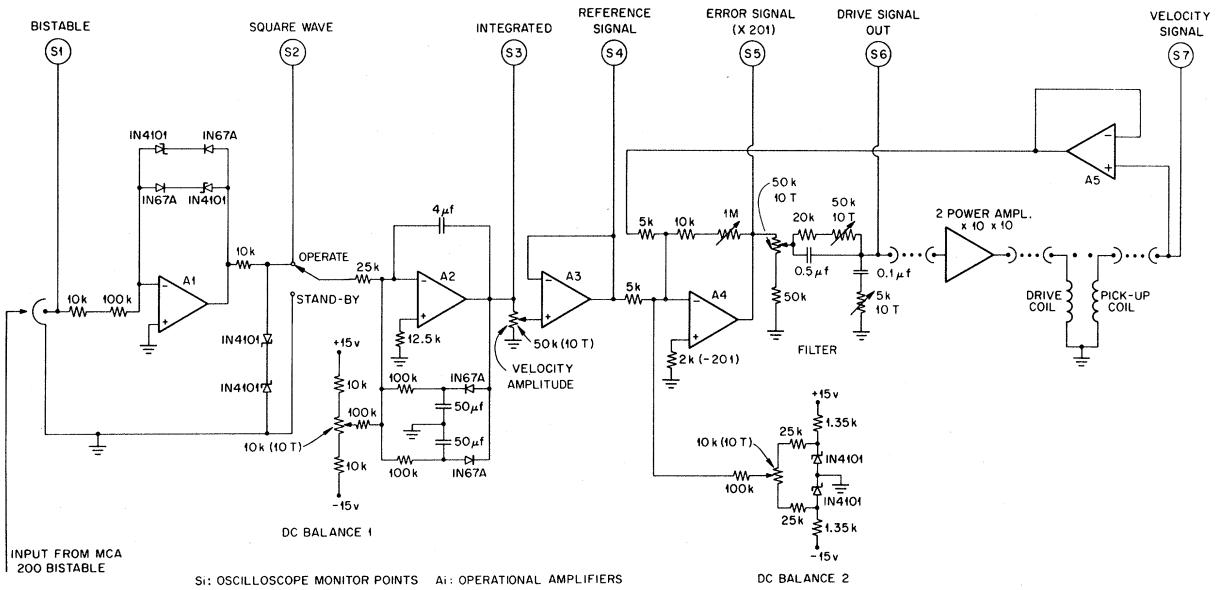

FIG. 2. Transducer control circuit.

sensor. The linearity of the reference signal is determined by the accuracy of the integrating circuit. An analysis of the expected computing errors of the integrator circuit (see Fig. 2), based on the specifications for the operational amplifier, showed that the largest error should be of the order of 10^{-4} nonlinearity due to finite gain at low frequencies. A measure of the nonlinearity due to (ii) was obtained from the ratio of the error voltage in the feedback loop to the reference voltage. This ratio was 0.1–0.2% (rms values) for the experiments reported here. The velocity sensor of the transducer contributed the major deviation from linearity of the spectrometer (~ 0.7)%.

Source and absorber were immersed in liquid helium in a glass cryostat. The absorber could be replaced while liquid helium was maintained in the Dewar. With count rates of about 10^5 counts/sec, spectra could be taken for two or three absorbers with a single source in spite of the short lifetime of ^{61}Co. The source-absorber-detector geometry is shown in Fig. 3. With a detector diameter of 5 cm, the solid angle was ~ 1%. Corrections due to reradiation from the absorber were less than 3.5% of the observed effect and unimportant compared to other uncertainties in determining recoilless fractions. The source was attached to the transducer with a thin-walled stainless-steel tube 75 cm long.

Mössbauer spectra, taken with a ^{57}Co in Cu source and a 25-μ Armco iron-foil absorber in this system, showed that the motion at the source position was in phase with the transducer motion. Linewidths of 0.21–0.24 mm/sec were typical for the inner lines of the spectrum.

C. Data Analysis

All spectra were fitted with a superposition of Lorentzian functions, the thin absorber approximation. The data stored in the two halves of the MCA memory, collected at opposite directions of motion, were fitted independently as was the folded spectrum. A comparison of the results of these three fits provided a measure for the linearity of the spectrometer. The spectral parameters (a) recoilless fraction, (b) magnetic hyperfine splitting, and (c) energy shifts were obtained from these Lorentz-line fits, except for some special cases which are described below.

a. Recoiless fraction. Values of the recoilless fraction were deduced from the areas of the absorption spectra. In the evaluation of the areas from the measured transmission spectra the influence of the experimental conditions must be taken into account.

The contribution of nonresonant background within the γ line which leads to a correction factor λ_γ = (total counts)/(signal counts) was determined periodically during the accumulation of a NGR spectrum. With high count rates the background fraction could be measured only approximately due to count-rate-dependent changes in the response of the γ spectrometer. The ensuing uncertainty of λ_γ of about 10% was the main source of error in the evaluation of the recoilless fraction.

Another factor that must be considered for NGR data accumulated at high count rates is the finite resolving time ρ of the counting instruments. If the

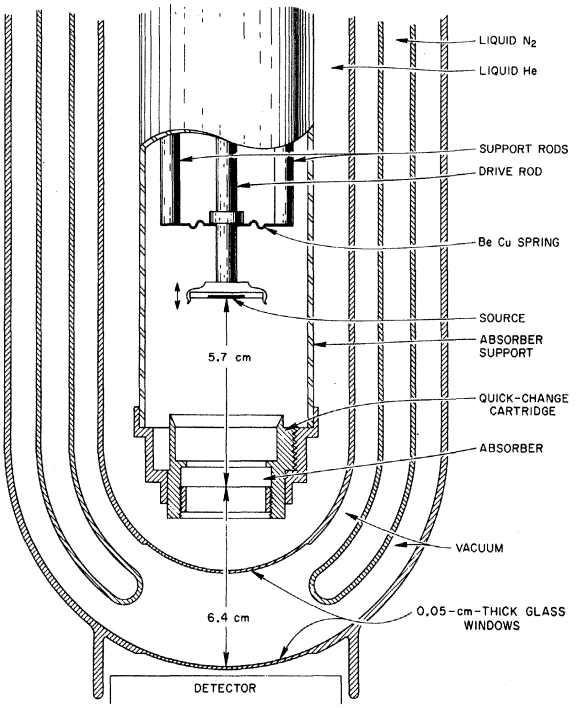

FIG. 3. Section through the bottom part of the liquid-helium cryostat showing source-absorber-detector geometry. The maximum displacement of the vibrating source from its center position was less than ±0.01 cm.

counting system is not paralyzed by high count rates so that ρ is a fixed dead time for each accepted pulse, the observed count rate n is related to the true rate N by $n = N/(1+N\rho)$.[33] Thus, relative changes of the count rate due to resonance absorption $(\delta N/N)$ lead to a measured effect, $(\delta n/n) = \lambda_c^{-1}(\delta N/N)$, where $\lambda_c = 1/(1-n\rho)$ if $(\delta N/N) \ll 1$.

The measured total absorption (= area) of every spectrum was multiplied by the factor $\lambda_{\text{total}} = \lambda_\gamma \lambda_c$.

For spectra with unresolved hyperfine splitting in absorbers of the thickness used in these experiments, the fit of the data with a superposition of Lorentz-shaped lines yielded excessively large values for the recoilless fraction f_A of the absorber. A simple way to retrieve this information lies in the application of the "Δ approximation"[34] which is appropriate for $M1$ transitions between high-spin states. An unresolved spectrum can be characterized by a dimensionless broadening parameter Δ which is defined as $\Delta(x) = [2\tau_N H_{\text{hf}}(x)/\hbar]\,|\mu_e - \mu_g|$. It depends on the magnetic moments μ_g and μ_e of the nuclear states, the mean life τ_N of the excited state, and the magnetic hyperfine field $H_{\text{hf}}(x)$ at the nuclei in environment x. A detailed description of the Δ approximation is given in Ref. 34.

The nuclear spins in the case of ^{61}Ni are near the limit of applicability of this approximation, and we have used the empirical value $\Delta(\text{Ni}) = 5$ for pure nickel, where $|H_{\text{hf}}(\text{Ni})| = (76 \pm 1)$ kOe.[35] For an absorber material x the value of $H_{\text{hf}}(x)$ was obtained by a Lorentz-line fit, and $\Delta(x)$ was estimated by assuming that $\Delta(x)/\Delta(\text{Ni})$ could be set equal to $H_{\text{hf}}(x)/H_{\text{hf}}(\text{Ni})$.

The effective thickness T_{eff} for the absorber was then found by graphical interpolation of the curves given in Fig. 4(c) of Ref. 34, employing this value of $\Delta(x)$ and the total absorption $\lambda_{\text{total}} F(x)$.

b. Magnetic hyperfine splitting. The recoilless emission or absorption spectra of ^{61}Ni in a magnetic field consist of 12 component lines (Fig. 1). The shape of the spectra and intensity ratios given in Refs. 1 and 24 for various experimental configurations were used in the analysis. Accurate values of the magnetic hyperfine fields were obtained from Lorentz-line fits.

In order to avoid possible systematic errors introduced by the superposition of Lorentzians in determining the magnetic moment of the 67.4-keV state of ^{61}Ni, we also fitted the spectra obtained for dilute solutions of Ni in Fe with the complete transmission integral and with six independent line positions. Both methods of fitting gave the same result for the ratio of the excited- and ground-state moments.

Other spectra were fitted with 12 Lorentzians and only two independent position parameters. From this fitting procedure we derive a centroid (energy shift) and a splitting parameter which is proportional to the average magnetic hyperfine field at the ^{61}Ni nuclei.

c. Energy shifts. Energy shifts observed for ^{61}Ni Mössbauer spectra are small. Therefore, it is necessary to ensure that instrumental distortions do not contribute significantly to the observed shifts. For this purpose Mössbauer spectra were taken with a 20-mC source of ^{57}Co in an iron foil, and an absorber taken from the same iron foil, and it was subjected to heat treatments together with the source. The relevant results of two spectra with different velocity amplitudes taken with this source-absorber combination at room temperature are presented in Table III. Instrumental distortions would give a constant shift when expressed in channels (Table III, column 2). The shift in velocity (Table III, column 3), which is independent of the conversion factor (column 1), indicates a real shift

TABLE III. Transducer zero-velocity calibration.

Velocity conversion [(μ/sec)/channel]	D [a] (channels)	Energy shift (μ/sec)
9.0	0.125 ± 0.046	−0.56 ± 0.21
13.5	0.076 ± 0.023	−0.51 ± 0.16

[a] $D = c_2 - c_1 - 200$; c_1 and c_2 are observed line centers in channels of first- and second-half spectra.

of the γ resonance.

The accuracy of energy-shift measurements of the ^{61}Ni spectra was limited by counting statistics which lead to standard deviations between 1 and 10 μ/sec for shift results.

IV. HYPERFINE INTERACTIONS IN 3d TRANSITION-METAL ALLOYS

A. Energy Shifts in Copper-Nickel Alloys

The parameters derived from Mössbauer spectra of ^{61}Ni in Cu-Ni alloy absorbers are given in Table IV. The concentration dependence of the observed energy shifts (with respect to the $^{64}Ni_{0.86}V_{0.14}$ source) can be described by $\delta(c) = (-1.2 + 19.2c)$ μ/sec, where c is the atomic fraction of copper.

Energy shifts of Mössbauer spectra arise from isomer shifts due to changes in electronic density and from second-order Doppler shifts (SOD) due to lattice motion. Source and absorber were in the same liquid-helium bath (4.2 °K); therefore thermal motions can be neglected and only the zero-point motions contribute to the SOD.

The SOD for a nucleus in a pure monatomic lattice is given in the harmonic approximation by the following integral over the phonon frequency distribution $g(\nu)$[36]:

$$\delta_{SOD} = (-h/2NMc)\int_0^\infty [\tfrac{1}{2} + (e^{\beta h\nu} - 1)^{-1}]\,\nu g(\nu)d\nu . \tag{3}$$

The logarithm of the recoilless fraction f may be expressed similarly:

$$\ln f = -(2R/3hN)\int_0^\infty [\tfrac{1}{2} + (e^{\beta h\nu} - 1)^{-1}]\,\nu^{-1} g(\nu)d\nu . \tag{4}$$

In these equations M is the mass of the Mössbauer nucleus, $\beta = 1/kT$, $R = E_\gamma^2/2Mc^2$, and $g(\nu)$ is normalized to $\int_0^\infty g(\nu)d\nu = 3N$, where $3N$ is the total number of normal modes of the crystal. These functions can be expressed in the limit of low temperatures in terms of the Debye moments ν_n of the frequency distribution[37]:

$$\nu_n \equiv \left|\tfrac{1}{3}(n+3)\mu_n\right|^{1/n}, \quad n \neq 0, \quad n > -3$$

where

$$\mu_n \equiv (1/3N)\int_0^\infty \nu^n g(\nu)d\nu .$$

For $T = 0$, Eqs. (3) and (4) become

$$\delta_{SOD} = -9h\nu_1/16Mc \tag{5}$$

and

$$\ln f = -3R/2h\nu_{-1} . \tag{6}$$

For $T = 4.2$ °K, the temperature-dependent terms omitted in Eqs. (5) and (6) amount to less than 0.1% of the leading terms quoted.

The distribution function $g(\nu)$ has been derived from neutron inelastic scattering data for Ni and Cu (Refs. 38 and 39, respectively). Our measurements are done with ^{61}Ni in these materials and we have to account for the difference in mass and force constants. The physical arguments for this impurity problem can be formulated in a simplified way: In the harmonic approximation, the normal-mode frequencies ν are related to the force constants γ and masses M by $\nu \propto (\gamma/M)^{1/2}$. Under the assumption that the impurity-host and host-host spring constants are equal, and for a mass ratio M(host)/M(imp) sufficiently close to unity that effects caused by localized modes of vibration may be neglected, effective moments for the impurity atoms can be calculated by

$$\nu_n(\text{imp}) = [M(\text{host})/M(\text{imp})]^{1/2}\nu_n(\text{host}).$$

The assumption of equal force constants certainly holds for ^{61}Ni in Ni. For the case of ^{61}Ni in Cu we can check the validity of this assumption by comparing the measured recoilless fraction $f = (11.1 \pm 1.0)\%$ with the calculated value $f = 11.5\%$.[40]

We summarize the relevant moments and Mössbauer parameters f and δ_{SOD} for ^{61}Ni in Ni and in Cu in Table V. The isomer shift $[\delta_{IS}(\text{Cu}) - \delta_{IS}(\text{Ni})]$ between ^{61}Ni in Cu and in Ni is then obtained by subtracting the relative SOD, $\delta_{SOD}(\text{Cu}) - \delta_{SOD}(\text{Ni}) = 14.0$ μ/sec from the measured shift $\delta_{expt}(\text{Cu}) - \delta_{expt}(\text{Ni}) = (+18.7 \pm 3.0)\,\mu$/sec. Thus, $\delta_{IS}(\text{Cu}) - \delta_{IS}(\text{Ni}) = (4.7 \pm 3.0)\,\mu$/sec.

Neutron scattering data about the lattice dynamics of concentrated Cu-Ni alloys were not available.

TABLE IV. Parameters of ^{61}Ni NGR spectra of Cu-Ni absorbers at $T = 4.2$ °K.

Ni concentration (at.%)	^{61}Ni thickness (mg/cm^2)	Total area (mm/sec)%	f (%)	Energy shift (μ/sec)	H_{hf} (kOe)
1.25	4.10	18.30±0.10	11.1±1.0	18.3±0.9	•••
2.5	5.20	23.14±0.22	13.0±1.0	16.2±2.5	•••
15	4.96	20.47±0.12	11.0±1.0	14.7±1.6	•••
30	5.42	21.36±0.15	10.8±1.0	12.2±1.3	•••
40	5.20	20.91±0.22	10.5±1.0	9.0±1.6	10±5
50	4.47	23.3±0.3	14.5±1.5	8.7±1.9	17±6
65	3.50	24.2±0.4	17.7±1.5	7.4±3.6	30±1
75	3.72	21.5±0.2	12.3±1.5	3.9±2.6	48±1
85	4.57	34 ±2	18.9±2.6	1.9±6.8	61±1
100	5.38	24.2±0.2	16.8±0.6	−0.4±3	76±1

TABLE V. Debye moments ν_n, SOD δ_{SOD}, and recoilless fractions f for ^{61}Ni in Ni and in Cu.

	Debye moments ν_n (10^{12} sec^{-1})		NGR parameter from ν_n (μ/sec)		Expt NGR parameters (μ/sec)
	From neutron[a] scattering	Effective moment for ^{61}Ni	δ_{SOD}	$\delta_{SOD}^{(Cu)} - \delta_{SOD}^{(Ni)}$	$\delta_{expt}^{(Cu)}$ $\delta_{expt}^{(Ni)}$
Ni	8.00	7.85	−96.7		
($n=1$)				+14.0	+18.7±3.0
Cu	6.57	6.71	−82.7		
			f(%)		f_{expt} (%)
Ni	8.08	7.93	16.4	...	16.8±0.6
($n=-1$)					
Cu	6.57	6.71	11.5	...	11.1±1.0

[a]The moment values for Cu were measured at 49 °K and for Ni at 296 °K (cf. Ref. 23).

Therefore, we have deduced δ_{SOD} for these alloys from our experimental f values, assuming that ν_1 equals ν_{-1}. As Table V shows, the two moments are equal within 1% both for pure Cu and for pure Ni. Since the uncertainty of the experimental f values is ~ 10%, small deviations from the assumed equality are not significant. The isomer shifts for the alloy system obtained by subtracting the SOD from the measured shifts are shown in Fig. 4. All isomer shifts are consistent with *zero*. The degree of sensitivity of these results to changes of the electronic structure upon alloying is indicated in the figure by the bands which correspond to the changes of the character of the electrons located at Ni atoms, marked at the respective bands.

B. Magnetic Hyperfine Fields in Ferromagnetic Alloys

We have measured the magnetic hyperfine splitting in ^{61}Ni in alloys of nickel with iron, cobalt, and copper. The values of H_{hf} for these alloys at $T = 4.2$ °K are listed in Table VI. Results for Ni-Fe alloys agree with those of Erich[26] and with NMR results.[41,42]

In these alloy systems, the concentration dependence of H_{hf} is very nearly proportional to that of the average magnetic moment per atom, $\bar{\mu}$. Since H_{hf} in pure nickel is known to be negative, it can be inferred from the smooth monotonic variation of the field with alloy concentration that H_{hf} is negative in all alloys investigated. These results fit into the over-all picture of hyperfine fields in ferromagnetic 3*d* metals discussed in detail by Shirley *et al.*[21]

In some alloys, particularly in $Fe_{0.3}Ni_{0.7}$ and in $Fe_{0.2}Ni_{0.8}$, a broadening of the outer lines relative to the inner ones indicates a distribution of magnetic hyperfine fields.[42]

The value of $|H_{hf}|$ for $Cu_{0.6}Ni_{0.4}$ is somewhat larger than expected from the general proportionality to $\bar{\mu}$. This could possibly be a consequence of clustering.[43]

The magnetic hyperfine field in pure nickel, $H_{hf}^{expt}(Ni) = (-76 \pm 1)$ kOe, can be compared with a calculation of the total unpaired spin density at nickel nuclei by Wakoh and Yamashita,[18] which gives a contact hyperfine field, $H_c = -147$ kOe. To this we add the positive orbital field estimated with the approximation, Eq. (12), and $\Delta g = 0.18$, $\langle S_z \rangle = 0.7$, and $\langle r^{-3} \rangle = 7.09$ a.u., to be $H_{orb} \cong +56$ kOe. The

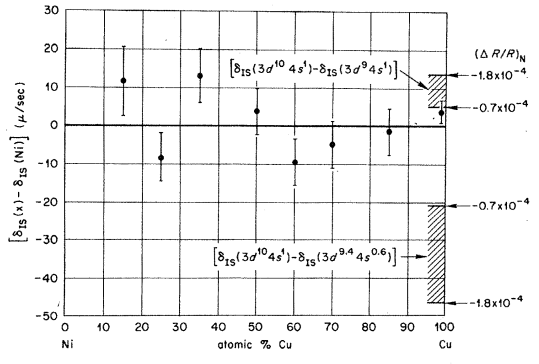

FIG. 4. Isomer shifts of ^{61}Ni NGR spectra in nickel-copper alloys as a function of copper concentration. Zero shift corresponds to pure nickel. The bands show the ranges of relative isomer shifts calculated for the indicated changes of the nickel electron configuration and the range $(\Delta R/R)_N$ determined in this experiment. A major contribution to the uncertainties of the experimental data shown is the uncertainty of the SOD in the alloys.

TABLE VI. Magnetic hyperfine fields at ^{61}Ni nuclei in ferromagnetic alloys of nickel with iron, cobalt, and copper.

Absorber	$\|H_{hf}\|$ (kOe)	Absorber	$\|H_{hf}\|$ (kOe)	Absorber	$\|H_{hf}\|$ (kOe)
		Pure Ni	76±1		
$Fe_{0.2}Ni_{0.8}$	135±15	$Ni_{0.85}Cu_{0.15}$	61±1	$Co_{0.1}Ni_{0.9}$	88±2
$Fe_{0.3}Ni_{0.7}$	165±15	$Ni_{0.75}Cu_{0.25}$	48±1	$Co_{0.3}Ni_{0.7}$	113±2
$Fe_{0.5}Ni_{0.5}$	200±2	$Ni_{0.65}Cu_{0.35}$	30±1	$Co_{0.5}Ni_{0.5}$	146±6
$Fe_{0.7}Ni_{0.3}$	209±5	$Ni_{0.5}Cu_{0.5}$	17±6		
$Fe_{0.95}Ni_{0.05}$	234±2	$Ni_{0.4}Cu_{0.6}$	10±5		
$Fe_{0.99}Ni_{0.01}$	234±2	$Ni_{0.3}Cu_{0.7}$	0±3		

result, $H_{hf}^{theoret}(Ni) = -91$ kOe, is reasonably close to the experimental value, $H_{hf}^{expt}(Ni) = -76$ kOe, in view of the many approximations involved in the derivation. The authors of Ref. 18 neglect the orbital field and compare their calculated value with an experimental result, $H_{hf}^{expt} = -170$ kOe, [44] which had been derived on the basis of a wrong determination of the magnetic moment of the ^{61}Ni ground state. [45]

V. IONIC NICKEL COMPOUNDS

For an interpretation of experimental isomer-shift data in terms of electronic structure, the difference of the nuclear charge radius between excited state and ground state must be known. This quantity could be obtained in principle from isomer-shift measurements with substances of known electronic configuration of the Mössbauer atoms. Ionic compounds usually fulfill this condition better than metallic materials. The electronic configuration is in some cases at least approximately that of the idealized charge state which can be used in conjunction with theoretically determined electronic wave functions in a first estimate of electronic charge densities at the nuclei. Overlap and covalent admixtures, especially of electronic states of s character, bring deviations and must be accounted for in a refinement of the analysis. [46]

The SOD, δ_{SOD}, whose magnitude is determined by the phonon spectra has to be subtracted from the observed energy shifts δ_{expt} to obtain the isomer shift δ_{IS}. Only in the limit of high temperatures $\delta_{SOD} \to -3kT/2Mc$ for all substances, and the relative SOD at a given temperature becomes very small. The relative isomer shift between resonance spectra of substances A and B is then given by

$$\delta_{IS}(A) - \delta_{IS}(B) = \delta_{expt}(A) - \delta_{expt}(B) - \delta_{SOD}(A) + \delta_{SOD}(B) . \quad (7)$$

Experimental information on the lattice dynamics of compounds with complicated structure is available only in a few exceptional cases. This restricts the selection of compounds which can be used for isomer-shift calibration.

In Table VII we summarize the characteristic parameters of ^{61}Ni Mössbauer spectra obtained with nickel-compound absorbers. Analysis of the energy shifts and the isomer-shift calibration will be discussed in Sec. V A and magnetic hyperfine fields in Sec. V B.

TABLE VII. Parameters of ^{61}Ni NGR spectra of nickel-compound absorbers at $T = 4.2$ °K.

Compound	Formal charge state	f_A(4.2 °K) (%)	Energy shift[a] (μ/sec)	$\lvert H_{hf} \rvert$ (4.2 °K) (kOe)
$K_4Ni_2(CN)_6$	+1	0.25±0.05	−34±10	...
NiF_2	+2	13.8±1.0	+19±2	45±1
$KNiF_3$	+2	14.8±1.3	+ 9±10	64±2
NiO	+2	11.5±1.1	+13±5	100±2
$NiSO_4 \cdot 7H_2O$	+2	0.32±0.05	+19±4	...
$(NH_4)_{12}[NiMo_9O_{32}]_2 \cdot 13H_2O$	+4	18.5±1.5	−81±6	...
NiAl	...	9.3±0.9	+24±3	...

[a] Total energy shift observed with respect to the $^{64}Ni_{0.86}V_{0.14}$ source.

A. Energy Shifts and Nuclear Charge Radii of ^{61}Ni

The phonon spectrum of a polyatomic crystal lattice with n atoms per unit cell consists of $3n$ branches. The frequency distribution of three of these branches (acoustic modes) can be approximated by a Debye spectrum. The frequency distributions of the other branches (optical modes) are narrow, and, neglecting dispersion, we will approximate them by δ functions. The expression for the frequency distribution $g(\nu)$ is then

$$g(\nu) = \frac{9N\nu^2}{n\nu_D^3}\Theta(\nu_D - \nu) + \frac{N}{n}\sum_{i=1}^{3(n-1)}\delta(\nu - \nu_i). \quad (8)$$

The normalization is the same as given following Eq. (4); ν_D is the cutoff frequency of the Debye spectrum.

This is the frequency distribution for vibrations of the entire lattice. For our calculations of properties associated with the vibrations of a particular atomic species, we have to know the partition of energies and amplitudes among the atoms forming the lattice. For this analysis we applied the formalism given by Housley and Hess. [47]

We introduce weight factors w_{ji} (b_{jli}^2 in the notation of Ref. 47) which are those fractions of the total vibrational energy of the ith normal mode associated with the motion of nickel atoms in direction j. The corresponding weight factor for the Debye spectrum which is assumed to be isotropic is denoted w_D. Thus, the total weight of the contribution of acoustic modes is $3w_D$. Using Eqs. (5) and (6) and the assumed frequency spectrum, Eq. (8), we can express the SOD δ_{SOD} and the logarithm of the recoilless fraction f in the low-temperature limit in the following way:

$$\delta_{SOD} = -\frac{9h w_D \nu_D}{16Mc} - \frac{h}{4Mc}\sum_{j,i} w_{j,i}\nu_i , \quad (9)$$

$$\ln f = -\frac{3R w_D}{2h \nu_D} - \frac{R}{3h}\sum_{j,i}\frac{w_{j,i}}{\nu_i} , \quad (10)$$

where

$$w_D + \textstyle\sum_i w_{j,i} = 1 \quad \text{for } j = x, y, z.$$

Optical-mode frequencies and the corresponding weight factors have been taken from detailed experimental investigations by infrared spectroscopy and concurrent theoretical model calculations on NiF_2 and $KNiF_3$. [48] For NiO only optical-mode fre-

quencies were available.[49] In this case we have used the approximate relation $w_D \approx M(\mathrm{Ni})/M(\mathrm{unit\ cell})$. The three optical modes were assumed to have equal weights, $w_{jt} = \frac{1}{3}(1 - w_D)$.

The parameters relating to the optical modes were substituted in Eq. (10), and ν_D could be deduced from the measured values of the recoilless fraction, given in Table VII. Then all parameters appearing in the expression for δ_{SOD} in Eq. (9) are known and the shift due to zero-point motions can be calculated. The uncertainty associated with this evaluation, including experimental errors of f values and approximations in the derivation, is about $\pm 5\ \mu$/sec.

For the other compounds listed in Table VIII, information on lattice dynamics was unavailable. We have obtained an estimate of the SOD by first calculating the shift expected in the framework of a Debye model $\delta_{\mathrm{SOD}}^{(\mathrm{Debye})} = +178/\ln f\ \mu$/sec, using the experimental values for f. For NiF_2, $KNiF_3$, and NiO this approach yields a number which lies between 80 and 83% of the shift calculated with explicit consideration of optical-mode vibrations. Thus, a better estimate of the SOD should be $\delta_{\mathrm{SOD}} = 1.23\,\delta_{\mathrm{SOD}}^{(\mathrm{Debye})}$. We estimate the uncertainty of SOD's calculated in this way to be $\pm 20\ \mu$/sec.

The decomposition of experimental energy shifts in terms of SOD and isomer shifts is displayed in Table VIII. In the analysis of energy shifts between absorbers and $^{64}Ni_{0.86}V_{0.14}$ alloy sources according to Eq. (7), we substitute for the SOD of the source the value deduced for pure Ni: $\delta_{\mathrm{SOD}}^{(\mathrm{NiV})} = -96.7\ \mu$/sec (Table V, column 4). This is justified by the fact that the measured recoilless fractions are the same for the two materials. In the following evaluation of $(\Delta R/R)_N$ we consider only shifts between ionic absorbers which are independent of our assumption for $\delta_{\mathrm{SOD}}^{(\mathrm{NiV})}$.

Since exact values of electronic charge densities at ^{61}Ni nuclei in the compounds investigated here were not available, we have attempted to find only limiting values for $(\Delta R/R)_N$.

TABLE VIII. Decomposition of experimental energy shifts of ^{61}Ni NGR spectra of nickel-compound absorbers.

Compound	δ_{expt}[a] (μ/sec)	$\delta_{\mathrm{SOD}}^{(A)}$ (μ/sec)	$\delta_{\mathrm{SOD}}^{(A)} + 97$ (μ/sec)	δ_{IS}[b] (μ/sec)
$K_4Ni_2(CN)_6$	-34 ± 10	-37	$+60$	-94 ± 23
NiF_2	$+19 \pm 2$	-112	-15	$+34 \pm 12$
$KNiF_3$	$+9 \pm 10$	-112	-15	$+24 \pm 12$
NiO	$+13 \pm 5$	-103	-6	$+19 \pm 9$
$NiSO_4 \cdot 7H_2O$	$+19 \pm 4$	-38	$+59$	-40 ± 21
$(NH_4)_{12}[NiMo_9O_{32}]_2 \cdot 13H_2O$	-81 ± 6	-138	-33	-48 ± 21
NiAl	$+24 \pm 3$	-92	$+5$	$+19 \pm 21$

[a] Total energy shift observed with respect to the $^{64}Ni_{0.86}V_{0.14}$ source.

[b] Isomer shift with respect to Ni, derived from δ_{expt} and $\delta_{\mathrm{SOD}}^{(A)} - \delta_{\mathrm{SOD}}^{(\mathrm{NiV})} = \delta_{\mathrm{SOD}}^{(A)} + 97$.

The most positive isomer shift was found in NiF_2. From this we can conclude that $(\Delta R/R)_N$ is negative. Then the electronic configuration at the nickel ions in NiF_2 is closer to the ideal one, $3d^8$, than in the other Ni^{2+} compounds (Fig. 5). We assume that for NiF_2 we can neglect deviations from the ideal configuration.

An upper limit for $|(\Delta R/R)_N|$ is obtained if we neglect 4s admixture in the Ni^{4+} complex where it is likely to be stronger than in NiF_2. The isomer shift between this material and NiF_2 is $\delta_{\mathrm{IS}}(Ni^{4+}) - \delta_{\mathrm{IS}}(NiF_2) = (-82 \pm 22)\mu$/sec. The largest contribution to the uncertainty of this value originates in the estimate of the SOD for Ni^{4+}. We use an excessive value $-104\ \mu$/sec to obtain the upper limit $|(\Delta R/R)_N|_{\max} = 1.8 \times 10^{-4}$ in conjunction with the computation of electronic charge densities for the configurations $3d^6$ and $3d^8$ (see Table I). In Fig. 5 we show the resulting isomer-shift scale marked by the value of $(\Delta R/R)_N$.

For the lower limit we use a minimum value $-104\ \mu$/sec of the uncertainty range of our result $\delta_{\mathrm{IS}}(Ni^{1+}) - \delta_{\mathrm{IS}}(NiF_2) = (-128 \pm 24)\ \mu$/sec. For the electronic configuration of Ni ions in $K_4Ni_2(CN)_6$ we make the extreme assumption $3d^8 4s^2$, which is compatible with the diamagnetism of this material,[50] and certainly overestimates the degree of covalency. This gives the lower limit $|(\Delta R/R)_N|_{\min} = 0.7 \times 10^{-4}$, and the second isomer-shift scale in Fig. 5.

We conclude that $(\Delta R/R)_N$ lies in the range $-1.8 \times 10^{-4} \leq (\Delta R/R)_N \leq -0.7 \times 10^{-4}$. The values for $(\Delta R/R)_N$ obtained by other groups,[26,51] -2.5 to -3.0×10^{-4}, are outside this range although not very far. The apparent agreement must be fortuitous since in some cases the major contribution to the measured energy shift (quoted as isomer shifts in Refs. 26 and 51) stems from the relative SOD, which seems to have slipped the attention of these authors.

The electronic charge density at nickel nuclei in metallic nickel has been calculated by Wakoh and Yamashita in the framework of nonrelativistic band theory.[18] If we multiply their value of the total electronic density by $S'(28) = 1.34$, we obtain $\rho_{\mathrm{el}}^{\mathrm{Ni}}(0) = 1349.0 \times 10^{26}$ cm^{-3}, a value which is far outside the range of densities calculated with the program RELWAV (see Table I). The difference lies in the densities of the core states with s character $\rho_{1s\text{-}3s}(0)$. For these states the calculation with Wigner-Seitz boundary conditions is a good approximation, and in order to obtain a basis for comparison of the shifts, we use the RELWAV result with $r_{WS} = 1.404 \times 10^{-8}$ cm for $3d^9 4s^1$: $\rho_{1s\text{-}3s}(0) = 1329.72 \times 10^{26}$ cm^{-3}. To this we add the 4s density derived from the calculation of Wakoh and Yamashita, $\rho_{4s}(0) = 0.54 \times 10^{26}$ cm^{-3} (including the factor 1.34). The total density is then $\rho_{\mathrm{el}}^{\mathrm{Ni}}(0) = 1330.26 \times 10^{26}$ cm^{-3}. This value agrees with the experimental result for nickel on the isomer-shift scale for $(\Delta R/R)_N = -0.7 \times 10^{-4}$

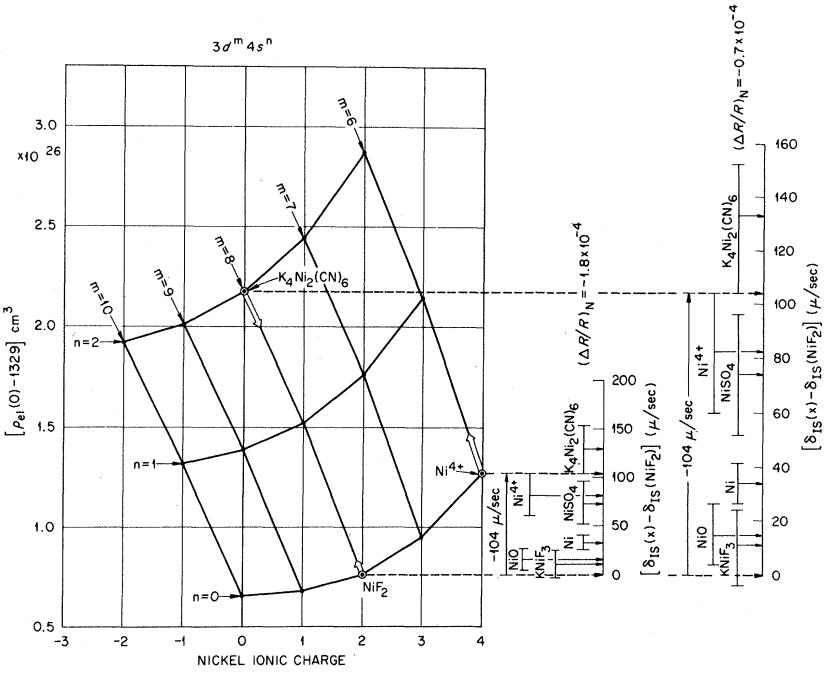

FIG. 5. Panek-Perlow plot of total electron densities calculated for the nickel configurations $3d^m4s^n$ in the framework of a relativistic Hartree-Slater-Latter approximation and with Wigner-Seitz boundary conditions at the radius $r_{WS} = 1.404\times10^{-8}$ cm. Densities for integer values of m and n were computed and are linearly interpolated. Isomer-shift scales shown to the right have been deduced from the indicated coordination of assumed electron configurations and experimental shifts for NiF_2, $(NH_4)_{12}[NiMo_9O_{32}]_2\,13H_2O$ (Ni^{4+}), and $K_4Ni_2(CN)_6$. The two scales represent extreme limits for the ^{61}Ni isomer-shift scale and limit the range of $(\Delta R/R)_N$.

(see Fig. 5). Core densities $\rho_{1s-3s}(0)$ for configurations between $3d^84s^0$ and $3d^{10}4s^1$ differ from the value quoted above at most by $\pm\,0.08\times10^{26}$ cm^{-3} and do not affect this comparison.

B. Magnetic Hyperfine Fields in Antiferromagnetic $3d^8$ Compounds

The dominant components of the magnetic hyperfine fields of transition-metal ions in magnetically ordered compounds[52] are the core-polarization field H_{cp}, the orbital field H_{orb}, and for ions at lattice sites of lower-than-cubic symmetry, the dipolar field. An additional contact field can arise from overlap and covalent mixing of ligand and metal 4s orbitals.

In Table IX we compare our experimental values of H_{hf} at ^{61}Ni nuclei in $KNiF_3$, NiO, and NiF_2 with calculations of H_{hf} based on the assumption that $H_{hf} = H_{cp} + H_{orb}$, neglecting other contributions.

For H_{cp} we use the approximation

$$H_{cp} = H_{cp}(S=1)\langle S_z\rangle\ . \qquad (11)$$

The value $H_{cp}(S=1) = -332$ kOe, calculated by Watson and Freeman for free Ni^{2+} ions, has been used in Table IX.

The expectation value of the spin $\langle S_z\rangle$ at a magnetic ion in a crystal with antiferromagnetic order is reduced from the free-ion value (for Ni^{2+} with configuration $3d^8$: $\langle S_z\rangle_{free\text{-}ion} = 1$) by two mechanisms[53]:

(a) Spin density is transferred to the ligand anions by covalent admixture and is compensated by an equal transfer of electrons with opposite spin to the ligand ion if it is coordinated with an even number of transition-metal ions. The reduction factor due to this effect is $[1-3(f_\sigma+f_s)]$, where f_σ and f_s are the fractions of unpaired electron spin transferred to the ligand $2p_\sigma$ and 3s orbitals, respectively.

(b) Zero-point motions of an antiferromagnetically ordered spin system in its ground state reduce the net average spin on any ion. This problem has been treated by Anderson[54] in the framework of a spin-wave model.

Measurements of $\langle S_z\rangle$ by neutron diffraction have been reported for $KNiF_3$[55] and for NiO.[56] In NiF_2 the spin density transferred to the ligand ions, $(f_\sigma+f_s) = 0.048$ has been measured by NMR of ^{19}F.[57] For the zero-point reduction factor we have used Anderson's[54] estimate for a simple cubic lattice with nearest-neighbor exchange interactions $\langle S_z\rangle/S = (1-0.078)$. NMR measurements have also been

TABLE IX. Magnetic hyperfine fields at ^{61}Ni nuclei in antiferromagnetic Ni^{2+} compounds. Symbols are defined in the text. Values in kOe unless otherwise noted.

	$KNiF_3$		NiO	NiF_2
Δg[a]	0.29		0.23	0.31
$\langle S_z\rangle$	0.85[b]	0.80[c]	0.81[b]	0.79[c]
$H_{cp} = -332\langle S_z\rangle$	−282	−266	−269	−262
$H_{orb} = 884\Delta g\langle S_z\rangle$	−218	205	165	217
$H_{hf}^{calc} = H_{cp} + H_{orb}$	−64	−61	−104	−45
$\lvert H_{hf}\rvert^{expt}$	64±2		100±2	45±1
$\langle r^{-3}\rangle_{expt}$[d] (a.u.)	5.5		5.6	5.3

[a] From Refs. 55, 59–61.
[b] Neutron diffraction results, Refs. 55 and 56.
[c] NMR measurements of (f_s+f_σ), Refs. 57 and 58.
[d] $\langle r^{-3}\rangle_{expt} = (-\lvert H_{hf}\rvert^{expt} + 275\langle S_z\rangle)/2\mu_B\Delta g\langle S_z\rangle$.

performed in $KNiF_3$ [58] and for comparison we include in Table IX an estimate of $\langle S_z \rangle$ based on these data and on Anderson's result.

The orbital field is given by

$$H_{\text{orb}} = \mu_B \langle r^{-3} \rangle \langle L_z \rangle \approx 2\mu_B \, \Delta g \langle r^{-3} \rangle \langle S_z \rangle \ . \qquad (12)$$

Here $\Delta g = g - 2.0023 \approx \langle L_z \rangle / 2\langle S_z \rangle$ is the shift of the Ni^{2+} g factor from the spin-only value. It is a measure of the unquenched orbital angular momentum which is introduced by spin-orbit coupling of the electronic levels in the crystal field. This parameter depends strongly on the covalent mixing of nickel e_g orbitals with $2s$ and $2p$ orbitals of the ligand anions. We use results of ESR measurements on Ni^{2+} impurity ions in nonmagnetic host lattices with the same ligand coordination as in the Mössbauer absorbers (for $KNiF_3$: $g = 2.29$, Ni^{2+} in $KMgF_3$, [59,55] and for NiO: $g = 2.23$, Ni^{2+} in MgO [60]). For NiF_2 we use the value $\bar{g} = 2.31$, deduced by Joenk and Bozorth[61] from their measurements of the magnetic susceptibility of NiF_2.

The value $\langle r^{-3} \rangle = 7.09$ a.u. has been calculated for Ni^{2+} ions by Freeman and Watson.[20]

If the sign of the fields measured in these antiferromagnetic compounds is negative, there is good agreement with the calculated values.

A major drawback of this comparison of the experimental fields with the theoretical calculations by Watson and Freeman[20,22] is the possibility of mutual cancellation of errors in the values for $H_{cp}(S=1)$ and for $\langle r^{-3} \rangle$. Thus, the consistent agreement that we have obtained with the quoted values is completely lost if we substitute $H_{cp}(S=1) = -275$ kOe, computed by Watson and Freeman[22] for Ni^{2+} ions in a cubic crystalline field (with parameters appropriate for NiO).

Our experimental data, in conjunction with this value for $H_{cp}(S=1)$, can be used to estimate $\langle r^{-3} \rangle$. The results, given as $\langle r^{-3} \rangle_{\text{expt}}$ in Table IX, agree reasonably well with the estimate of $\langle r^{-3} \rangle = 5.8$ a.u. obtained by Watson and Freeman[22] through interpolation of experimental data for Co^{2+} and Cu^{2+} by Abragam, Horowitz, and Pryce.[62]

The problem of covalency in $KNiF_3$ has been treated theoretically by Hubbard, Rimmer, and Hopgood with the configuration interaction method,[63] including admixtures of $4s$ electrons at Ni^{2+} ions. From their results and the electron densities given in Table I we calculate an isomer shift of -2 to $-5\,\mu$/sec [depending on the value of $(\Delta R/R)_N$] with respect to the configuration $3d^8$, and a contact hyperfine field due to $4s$ electrons of $+2$ kOe. The covalent $3d$ admixture leads to an isomer shift in the opposite direction whose absolute value is about one-third of the $4s$ shift.

The local symmetry of Ni^{2+} sites in NiF_2 is not cubic. A weak dipolar field due to nearest-neighbor cations is estimated to be -3 kOe.[57] The lower symmetry also leads to an electric field gradient at ^{61}Ni nuclei in NiF_2, and the spectrum shown in

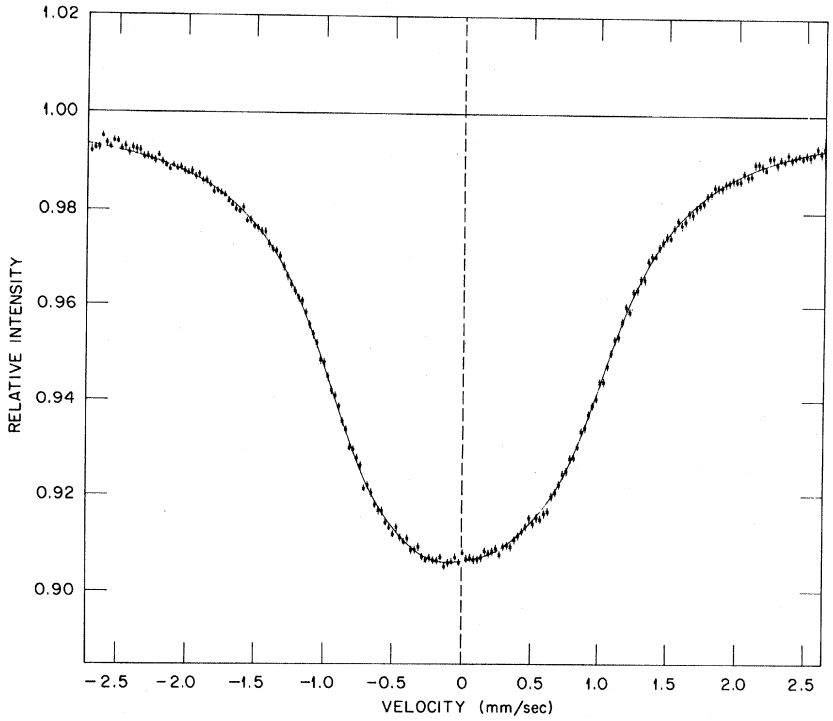

FIG. 6. Mössbauer spectrum obtained with the source ^{61}Co in a nonmagnetic $^{64}Ni_{0.86}V_{0.14}$ alloy, and a NiF_2 absorber at 4.2 °K showing both magnetic dipole and a weak electric quadrupole hyperfine interaction in the absorber. In the fitting procedure we assumed an axial electric-field-gradient tensor and that the magnetic field is parallel to the principal axis to the field-gradient tensor.

Fig. 6 could not be fitted with the assumption of magnetic splitting only. The poor resolution of the spectral lines prevented a complete determination of the electric-field-gradient tensor and its orientation with respect to the magnetic field direction. However, the spectrum could be fitted with the assumption of an axial field gradient whose axis is parallel to the magnetic field. The magnitude obtained for the quadrupole interaction energy for the ^{61}Ni ground state is $e^2qQ_g = (10 \pm 8) \times 10^{-9}$ eV.

ACKNOWLEDGMENTS

It is a pleasure to acknowledge many fruitful discussions with J. O. Thomson, H. H. F. Wegener, and E. O. Wollan and to thank them for their interest in this work. We are also indebted to T. C. Tucker and J. D. Proffitt for the calculation of Hartree-Fock-Slater wave functions, D. E. LaValle for the preparation and analyses of the materials, and J. Burton for the program for fitting the transmission integral to experimental Mössbauer spectra.

*Research sponsored by the U.S. Atomic Energy Commission under contract with the Union Carbide Corp.

†Oak Ridge Graduate Fellow from Ohio State University under appointment with Oak Ridge Associated Universities. Based on a thesis submitted to Ohio State University in partial fulfillment of the requirements for the Ph. D. degree. Present adress: Clarkson College of Technology, Potsdam, N. Y. 13676.

‡Present address: Kernforschungszentrum, Karlsruhe, Germany.

[1]F. E. Obenshain and H. H. F. Wegener, Phys. Rev. 121, 1344 (1961).

[2]L. R. Walker, G. K. Wertheim, and V. Jaccarino, Phys. Rev. Letters 6, 98 (1961).

[3]J. Danon, in *Chemical Applications of Mössbauer Spectroscopy*, edited by V. I. Goldanskii and R. H. Herber (Academic, New York, 1968), p. 160.

[4]T. A. Kitchens, W. A. Steyert, and R. D. Taylor, Phys. Rev. 138, A467 (1965).

[5]G. K. Wertheim and J. H. Wernick, Phys. Rev. 123, 755 (1961); B. Window and C. E. Johnson, Phys. Letters 29A, 703 (1969).

[6]L. D. Roberts, R. L. Becker, F. E. Obenshain, and J. O. Thomson, Phys. Rev. 137, A895 (1965).

[7]A. E. Balabanov and N. N. Delyagin, Fiz. Tverd. Tela 9, 1899 (1967) [Soviet Phys. Solid State 9, 1498 (1968)].

[8]Rigid-band model: N. F. Mott, Proc. Phys. Soc. (London) 47, 571 (1935); minimum-polarity model: N. D. Lang and H. Ehrenreich, Phys. Rev. 168, 605 (1968); coherent-potential approximation: S. Kirkpatrick, B. Velický, and H. Ehrenreich, Phys. Rev. B 1, 3250 (1970).

[9]F. E. Obenshain, J. C. Love, and G. Czjzek, in *Proceedings of the Eleventh International Conference on Low-Temperature Physics, St. Andrews, Scotland*, 1969, edited by J. F. Allen, D. M. Finlayson, and D. M. McCall (St. Andrews U. P., St. Andrews, Scotland, 1968), p. 532; J. C. Love, F. E. Obenshain, and G. Czjzek, Bull. Am. Phys. Soc. 14, 345 (1969).

[10]M. E. Rose, *Multipole Fields* (Wiley, New York, 1955).

[11]A. J. F. Boyle and H. E. Hall, Rept. Progr. Phys. 25, 441 (1962).

[12]D. A. Shirley, Rev. Mod. Phys. 36, 339 (1964).

[13]S. Bernow, S. Devons, I. Duerdoth, D. Hitlin, J. W. Kast, E. R. Macagno, J. Rainwater, K. Runge, and C. S. Wu, Phys. Rev. Letters 18, 787 (1967).

[14]R. E. Watson, Solid State and Molecular Theory Group, MIT Technical Report No. 12 (unpublished).

[15]F. Herman and S. Skillman, *Atomic Structure Calculations* (Prentice-Hall, Englewood Cliffs, N. J., 1963).

[16]L. W. Panek and G. J. Perlow, ANL Report No. ANL-7631, 1969 (unpublished).

[17]T. C. Tucker, L. D. Roberts, C. W. Nestor, Jr., T. A. Carlson, and F. B. Malik, Phys. Rev. 178, 998 (1969).

[18]S. Wakoh and J. Yamashita, J. Phys. Soc. Japan 25, 1272 (1968).

[19]D. E. Ellis, A. J. Freeman, and P. Ros, Phys. Rev. 176, 688 (1968).

[20]A. J. Freeman and R. E. Watson, in *Magnetism*, edited by G. T. Rado and H. Suhl (Academic, New York, 1965), Vol. IIA, p. 167.

[21]D. A. Shirley, S. S. Rosenblum, and E. Matthias, Phys. Rev. 170, 363 (1968).

[22]R. E. Watson and A. J. Freeman, Phys. Rev. 120, 1125 (1960); 120, 1134 (1960).

[23]A. H. Muir, Jr., K. J. Ando, and H. M. Coogan, *Mössbauer Effect Data Index* 1958–1965 (Interscience, New York, 1966), p. 106.

[24]H. H. F. Wegener and F. E. Obenshain, Z. Physik 163, 17 (1961).

[25]L. E. Drain, Phys. Letters 11, 114 (1964). The standard error of the actual measurement was much less than the uncertainty quoted here where we include an uncertainty for the amount of diamagnetic shielding.

[26]U. Erich, Z. Physik 227, 25 (1969).

[27]J. C. Love, G. Czjzek, J. J. Spijkerman, and D. K. Snediker, in *Hyperfine Structure and Nuclear Radiations*, edoted by E. Matthias and D. A. Shirley (North-Holland, Amsterdam, 1968), p. 124; U. Erich and D. Quitmann, *ibid.*, p. 130.

[28]W. J. Childs and L. S. Goodman, Phys. Rev. 170, 136 (1968).

[29]A. Migdal, in *Many-Body Description of Nuclear Structure and Reactions*, edited by C. Bloch (Academic, New York, 1966), p. 171; the calculated value $-0.73\mu_N$ of the ^{61}Ni ground-state moment has been published by V. L. Birbrair, G. M. Gusinskii, V. I. Isakov, and I. Kh. Lemberg, Izv. Akad. Nauk SSSR, Ser. Fiz. 31, 1696 (1967) [Bull. Acad. Sci. USSR, Phys. Ser. 31, 1736 (1968)].

[30]R. A. Uher and R. A. Sorensen, Nucl. Phys. 86, 1 (1966). The model gives $(\Delta R/R)_N = -1.3 \times 10^{-4}$ for ^{61}Ni; R. A. Uher (private communication).

[31]E. N. Shipley, R. E. Holland, and F. J. Lynch, Phys. Rev. 182, 1165 (1969).

[32]E. Kankeleit, Rev. Sci. Instr. 35, 194 (1964).

[33]R. D. Evans, *The Atomic Nucleus* (McGraw-Hill, New York, 1955), Chap. 28, p. 785ff.

[34]G. Czjzek, J. L. C. Ford, J. C. Love, F. E. Obenshain, and H. H. F. Wegener, Phys. Rev. 174, 331 (1968).

[35]This value of Δ(Ni) gave consistent results for spectra of two nickel absorbers with the thickness ratio 2:1. A later evaluation of these spectra with a fit of the complete

transmission integral gave a value for the recoilless fraction which was in agreement with that obtained by this procedure.

[36]H. H. F. Wegner, *Der Mössbauer-Effekt* (Bibliographisches Institut, Mannheim, 1965), pp. 61 and 109.

[37]L. S. Salter, Advan. Phys. 14, 1 (1965).

[38]R. J. Birgeneau, J. Cordes, G. Dolling, and A. D. B. Woods, Phys. Rev. 136, A1359 (1964).

[39]R. M. Nicklow, G. Gilat, H. G. Smith, L. J. Raubenheimer, and M. K. Wilkinson, Phys. Rev. 164, 922 (1967); R. M. Nicklow (private communication).

[40]Neutron scattering measurements reported by M. Sakamoto and Y. Hamaguchi, in *Proceedings of the Fourth IAEA Symposium on Neutron Inelastic Scattering*, Vol. 1 (International Atomic Energy Agency, Vienna, 1968), p. 181, showed anomalies of phonon-dispersion curves in Cu-Ni alloys which the authors interpreted as being caused by differences in force constants. Later measurements by B. N. Brockhouse (private communication) did not verify these anomalies.

[41]R. L. Streever, L. H. Bennett, R. C. LaForce, and G. F. Day, J. Appl. Phys. 34, 1050 (1963).

[42]T. J. Burch, J. I. Budnick, and S. Skalski, Phys. Rev. Letters 22, 846 (1969).

[43]B. Mozer, D. T. Keating, and S. C. Moss, Phys. Rev. 175, 868 (1968); T. J. Hicks, B. Rainford, J. S. Kouvel, G. G. Low, and J. B. Comly, Phys. Rev. Letters 22, 531 (1969).

[44]L. J. Bruner, J. I. Budnick, and R. J. Blume, Phys. Rev. 121, 83 (1961).

[45]J. W. Orton, P. Auzins, and J. E. Wertz, Phys. Rev. 119, 1691 (1960).

[46]E. Šimánek and Z. Šroubek, Phys. Rev. 163, 275 (1967); E. Šimánek and A Y. C. Wong, *ibid.* 166, 348 (1968).

[47]R. M. Housley and F. Hess, Phys. Rev. 146, 517 (1966).

[48]M. Balkanski, P. Moch, and G. Parisot, J. Chem. Phys. 44, 940 (1966); I. Nakagawa, A. Tsuchida, and T. Shimanouchi, *ibid.* 47, 982 (1967).

[49]P. J. Gielisse, J. N. Plendl, L. C. Mansur, R. Marshall, S. S. Mitra, R. Mykolajewycz, and A. Smakula, J. Appl. Phys. 36, 2446 (1965).

[50]L. Szegö and P. Ostinelli, Gazz. Chim. Ital. 60, 946 (1930); R. S. Nyholm, Proc. Chem. Soc., 273 (1961).

[51]J. C. Travis and J. J. Spijkerman, in *Mössbauer Effect Methodology*, edited by I. J. Gruverman (Plenum, New York, 1968), Vol. 4, p. 237.

[52]P. R. Locher and S. Geschwind, Phys. Rev. Letters 11, 333 (1963).

[53]J. Owen and J. H. M. Thornley, Rept. Progr. Phys. 29, 675 (1966).

[54]P. W. Anderson, Phys. Rev. 86, 694 (1952).

[55]M. T. Hutchings and H. S. Guggenheim, J. Phys. 3, 1303 (1970).

[56]B. E. F. Fender, A. J. Jacobsen, and F. A. Wedgewood, J. Chem. Phys. 48, 990 (1968).

[57]R. G. Shulman, Phys. Rev. 121, 125 (1961).

[58]R. G. Shulman and S. Sugano, Phys. Rev. 130, 506 (1963).

[59]T. P. P. Hall, W. Hayes, R. W. H. Stevenson, and J. Wilkens, J. Chem. Phys. 38, 1977 (1963).

[60]W. Low, Phys. Rev. 109, 247 (1958).

[61]R. J. Joenk and R. M. Bozorth, in *Proceedings of the International Conference on Magnetism, Nottingham, England*, 1964 (The Institute of Physics and The Physical Society, London, 1965), p. 493.

[62]A. Abragam, J. Horwitz, and M. H. L. Pryce, Proc. Roy. Soc. (London) A230, 169 (1955).

[63]J. Hubbard, D. E. Rimmer, and F. R. A. Hopgood, Proc. Phys. Soc. (London) 88, 13 (1966).

PHYSICAL REVIEW B VOLUME 3, NUMBER 9 1 MAY 1971

Satellite Free-Induction Signals in CdS:Mn

W. B. Mims

Bell Telephone Laboratories, Murray Hill, New Jersey 07974

(Received 1 December 1970)

Satellite free-induction signals occurring $\sim\frac{1}{4}$ μsec after the main free-induction signal have been observed during pulsed microwave experiments with Mn^{2+} in CdS. These signals also appeared flanking the echo in an electron spin-echo experiment and were ~60 times weaker than the spin echo itself. When the Zeeman field was swept, the phase of the satellite signals underwent alternations, returning to any given value each time the field was changed by ~1.4 G. It is shown that these satellites originate in the superhyperfine interaction of Mn^{2+} with the nuclei Cd^{111} and Cd^{113}. The ease with which the satellites could be observed in spite of heavy broadening of the superhyperfine spectrum suggests that this may be a useful way of studying contact interactions in cases where the interaction is too weak to give a clearly resolved spectrum.

During recent electron spin-echo experiments performed with a sample of CdS doped with Mn, a group of unfamiliar satellite signals were observed in the vicinity of the applied pulses and the echo. These signals appeared ~$\frac{1}{4}$ μsec after the two applied pulses and ~$\frac{1}{4}$ μsec on either side of the spin echo (see Fig. 1). When allowance was made for phase-memory decay, it was found that all these satellites were more or less comparable in amplitude. The satellites on either side of the echo were,